

# Uncertainty quantification/propagation in nonlinear models: robust reduction - generalized polynomial chaos

## 1. INTRODUCTION

In order to design large-scale engineering systems, especially in structural dynamics, it is necessary to use numerical models including uncertainties that can realistically describe the behavior of the system. With special emphasis on probabilistic framework ((Chiang et al. 1987), (Soize 2010)) and parametric uncertainties (e.g., material properties, geometry, boundary conditions, excitations), one can use stochastic uncertainty propagation methods (UPMs) to evaluate the effect of the randomness in structural input parameters, modeled with random variables, on the dynamic response of a system which varies also randomly. This randomness is quantified through post-process parameters such as static moments, probability density function (PDF) and probability of failure for structural reliability analysis and importance measures and sensitivity indices for sensitivity analysis. The sample-based UPMs, such as Monte Carlo Simulations (MCS) (Rubinstein 2008) and Latin Hypercube Sampling (LHS) (Helton and Davis 2003), are frequently used and considered as reference since they permit to achieve a reasonable accuracy. Nevertheless, they may be computationally unaffordable since the accuracy level is proportional to the number of generated deterministic simulations. As an alternative, among other non-sample-based UPMs, the generalized Polynomial Chaos Expansion (gPCE) method ((Wiener 1938), (Xiu and Karniadakis 2002), (Soize and Ghanem 2004)) requires a lower computational cost. Its expansion combines multivariate polynomials and deterministic coefficients which are computed using intrusive or non-intrusive approaches. The former entails model modifications (e.g. Stochastic Spectral FE method (SSFEM) (Ghanem and Spanos 1991)). However the latter

proves to be better by considering the FE model as a black box. The regression approach (Berveiller et al., 2006) and the Probabilistic Collocation Method (PCM) (Blanchard et al., 2009) are the most commonly used non-intrusive methods. Focusing on the former, a set of successive evaluations is generated to entail exact analyses of the full FE model.

gPCE has recently shown a growing emphasis and several works focused on its applications, both in uncertainty ((Ben Souf et al. 2015), (Dell'Elce and Kerschen 2015), (Hayes and Marques 2015), (Sinou et al. 2015), (Guerine et al. 2016)) and sensitivity analysis ((Dubreuil et al. 2014), (Perko et al. 2014), (Sudret and Mai 2015), (Deman et al. 2016)). Many variants enhancing the gPCE efficiency are also proposed. For example, a Time-Dependent gPC (TD-gPC) method was introduced by Gerritsma et al. (Gerritsma et al. 2010) to enhance the convergence of the gPC, which tends to break down for long-time integration, by considering that the PDF changes as a function of time. The Multi-Element gPC (ME-gPC) approach ((Wan and Karniadakis 2005), (Chouvion and Sarrouy 2016)) is based on an adaptive partitioning of the stochastic space to solve nonlinear problems with long-term integration difficulties. Recently, a non-intrusive metamodel called PC-Kriging has been introduced by Schobi et al. (Schobi et al. 2015). It is based on a least-square minimization algorithm selecting the optimal sparse set of polynomials with Kriging, which manages the local variability of the model output assumed to behave as a realization of a Gaussian random process. Recently, a convergence accelerator of the first two moments of the gPCE responses based on Aitken's transformation has been proposed in (Jacquelin et al. 2015). The work performed by Jacquelin et al. (Jacquelin et al. 2016) proves that fuzzy variables can also be expanded in terms of gPC when Legendre polynomials are used.

Despite the computational time reduction enabled by these methods with respect to the sample-based methods, direct dynamic analysis remains very cumbersome especially when large-

scale FE models, uncertainties, nonlinearities, etc. are considered. To overcome this challenge, this paper is focused on constructing computational metamodels combining UPMs and robust reduced order models (ROM) which must be properly used to reach satisfactory robustness against both parametric uncertainties and localized nonlinearities.

Several ROMs were introduced in the literature to deal with structural modifications including parameter perturbations and/or localized nonlinearities. A special emphasis is, here, put on weakly nonlinear dynamic systems when only localized nonlinearities are considered. In this context, the most frequently used ROMs are the Proper Orthogonal Decomposition (POD) ((Liang et al. 2002), (Kerschen et al. 2005)) and its variants (e.g. Smooth Orthogonal Decomposition) (Lulf et al. 2013), the combined approximations method (Kirsh 2000) and its variant introduced by Guedri et al. (Guedri et al. 2010), Krylov subspaces methods (e.g. Arnoldi, Gram-Schmidt and Lanczos) (Nour and Clough 1983), nonlinear normal modes (NNMs) (Kuether et al. 2014), recurrent artificial neural networks (ANN) (Yao and Liou 2012), and reduction basis generated by Ritz vectors or/and linear normal modes and enriched using static residual vectors (Balmès 1996a), etc.

This work deals with ROMs which use enriched Ritz or/and normal mode bases with static residual vectors. These ROMs can be made within two configurations: first-level ROMs, which are based on direct reduction technique, and  $n^{\text{th}}$ -level ROMs, which are extended to the component mode synthesis (CMS) approaches (Ohayon and Soize 2014). The later allow enriching and reducing the components (substructures) being uncertain and/or containing localized nonlinearities independently of the others. In the literature, enriching Ritz basis with static contribution of neglected eigenvectors was proposed in ((Balmès 1996a), (Bouazzouni et al. 1997)) for accurately evaluating frequency response of modified structures and extended to

CMS in (Balmès 1996b) and in (Masson et al. 2006). Bouazizi et al. (Bouazizi et al. 2006) associated the equivalent linearization method with a reduction basis enriched by static residual vectors accounting for parametric modifications and localized nonlinearities. CMS methods were extended by Wenneker et al. (Wenneker and Tiso 2014) to account for geometric nonlinearities by adding the properly chosen modal derivatives, describing second order nonlinear contributions of vibration modes perturbed with the shapes of some others. Among other CMS approaches, the Craig-Bampton CMS (CB-CMS) method (Craig and Bampton 1968) is the most frequently used. For instance, the enriched CB-CMS was associated with a hybrid design optimization method (Perdahcioglu et al. 2009) to study a fuselage structure with parameter modifications. Its efficiency was also proven in (De Lima et al. 2010) through its application to large FE models of industrial structures incorporating modified viscoelastic zones.

The aim of this study is to develop two metamodels combining gPCE and first-level ROM and second-level ROM, respectively. The proposed metamodels are tested in the determination of the time responses of a frame structure and a periodic coupled micro-beams structure, respectively. Both structures contain stochastic parameters and localized nonlinearities. The efficiency of the proposed metamodels is evaluated with respect to reference solutions obtained by using the LHS method on the whole FE model. Numerical results prove the efficiency of the proposed approach.

## 2. PROPOSED METAMODELS

Within the context of combining UPMs and ROMs, robust metamodels are introduced in this section. In the literature, several researches deal with combining ROMs and UPMs. For instance, the enriched CMS method was combined with the SSFEM, in (Guedri et al. 2006), to

compute frequency response of linear structures. The POD was combined with Galerkin method in (Weickum et al. 2009) to approximate the transient response of linear structures with random design parameters. In (Maute et al. 2009), a ROM is integrated into SSFEM using a basis spanned by displacements and derivatives of displacements, and implemented to optimize the shape of a linear shell structure. The CB-CMS was coupled in (Hinke et al. 2009) with perturbation techniques. The authors prove that the further level (component level) allowed by the CMS hence additional paths through which uncertainty propagates. Deterministic components do not require reanalysis, while stochastic ones can be treated independently. CMS methods were coupled with adaptive PCE (Sarsri et al. 2011) in order to investigate frequency transfer functions for large FE systems with linear and nonlinear stochastic parameters. Gauvar (Gaurav et al., 2011) proposed a method which consists on separating the nonlinear and/or stochastic system degrees or freedom (dofs) from the linear deterministic ones and, then, on using a non-standard form of a Nonlinear Volterra Integral Equation (NVIE) to calculate modification terms added to the nominal linear response to obtain the system response. The MCS method was implemented to analyze uncertainties. In order to obtain robust and reliable designs of nonlinear trusses problems, POD method was incorporated in a Multi-objective optimization (MO) (Afonso and Motta 2013) based on MCS and probabilistic collocation method (PCM). Raisee et al. (Raisee et al. 2013) developed a non-intrusive stochastic ROM for PC representation based on an adapted POD and a modified Karhunen-Loève expansion, in order to solve stochastic steady-state heat diffusion problem. Mohammadali et al. (Mohammadali and Ahmadian 2014) associated a linearized ROM over localized nonlinear regions to the HBM to solve nonlinear systems with localized nonlinearities under periodic motion. MO techniques are combined, in (Motta et al. 2015), with a

metamodel coupling the PCM and a reduced basis method (RBM) whose efficiency is evaluated through a posteriori error estimators and an effective off-line/on-line computational strategy.

The two robust metamodels proposed in this paper combine gPCE and two ROMs using enriched bases and are introduced in two ways. A first-level ROM is integrated into the gPCE regression technique by projecting the successive deterministic responses on an enriched basis (Section 2.2). Then, the ROM is extended to the CB-CMS method in order to apply a second-level ROM limiting the basis enrichment to the components with stochastic parameters and/or localized nonlinearities (Section 2.3).

## 2.1. Generalized Polynomial Chaos Expansion (gPCE)

In this study the gPCE method is used to approximate the solution of nonlinear mechanical systems which can generally be represented in the time domain by the differential equation

$$\begin{cases} M \ddot{y} + B \dot{y} + f_{int}(y) = f_{ext} \\ y(t_0) = y_0 \\ \dot{y}(t_0) = \dot{y}_0 \end{cases} \quad (1)$$

where the internal forces vector is of the form

$$f_{int} = (K + f_{NL}(y, \dot{y}))y \quad (2)$$

$K$ ,  $M$  and  $B$  stand for the stiffness, mass and damping matrices of the system while  $f_{ext}$  is the exciting forces vector.

The gPCE of second order random variables approximate the solution  $y$  of Eq.(1) using a decomposition, practically truncated by retaining only terms of the polynomials with degree up to  $p$ , of the form

$$\tilde{Y} = \sum_{j=0}^P \tilde{y}_j \Phi_j(\xi) = \tilde{\mathbf{y}}^T \Phi(\xi); \quad P + 1 = \frac{(d+p)!}{d!p!} \quad (3)$$

where  $\tilde{y}_j$  are the unknown deterministic coefficients and  $\Phi_j$  the multivariate polynomials of  $d$  independent random variables  $\xi = \{\xi_i\}_{i=1}^d$ .

Solving the gPCE consists on computing the deterministic coefficients  $\tilde{y}_\alpha$ . Hence, the non-intrusive regression method is implemented, in its standard form, minimizing the difference between the gPCE approximate solution and the exact solution consisting on a set of computed deterministic responses  $\{y(\xi^{(n)}), n = 1, \dots, N\}$  corresponding to  $N$  realizations of random variables  $\Xi = \{\xi^{(n)}\}_{n=1}^N$  forming an experimental design (ED). The approximate solution takes, consequently, the form

$$\tilde{y} = (\Phi^T \Phi)^{-1} \Phi^T y = \Phi^+ y \quad (4)$$

where  $\Phi_{nj} \equiv \left( \Phi_j(\xi^{(n)}) \right)_{\substack{n=1, \dots, N \\ j=0, \dots, P}}$  is called the data matrix and  $\Phi^+$  is its pseudo-inverse.

A necessary condition for the numerical stability of regression approximation consists on the selection of an ED of size  $N \geq P + 1$  in order to ensure the well-conditioning of the matrix  $(\Phi^T \Phi)$  to be inverted. In the literature, the ED is selected in two ways: (i) randomly with respect to probability distribution of random variables; (ii) deterministically among Hermite polynomial roots combinations. Some deterministic selection techniques are proposed in ((Berveiller et al. 2006), (Sudret 2008)). In this work, the roots of the Hermite polynomial of degree  $p + 1$  are at first computed, then all their possible combinations  $(p + 1)^d$  are calculated and finally these roots combinations are classified so that the following variable

$$\zeta_N(\xi^{(n)}) = 2\pi^{-d/2} \exp\left(-\frac{1}{2} \|\xi^{(n)}\|^2\right) \quad (5)$$

is maximized or  $\|\xi^{(n)}\|^2$  minimized in order to ensure that they are closest to the origin. The classified roots combinations are subject to another selection technique (Blatman and Sudret

2010). Indeed, to ensure that the invertible matrix  $(\Phi^T \Phi)$  is well-conditioned, a condition number  $\kappa$  defined as

$$\kappa = \|(\Phi^T \Phi)^{-1}\| \cdot \|\Phi^T \Phi\| \quad (6)$$

must be minimized, where  $\|\cdot\|$  is the 1-norm of the matrix. A number  $N$  of roots combinations, which verify Eq. (5), corresponds to the smallest value of  $\kappa$  and thus create the ED.

Once obtained, the coefficient estimates gives the final gPCE, Eq. (3). Statistical quantities, such as the first and second moments (the mean and the variance, respectively), could then be calculated to quantify the randomness of the stochastic response.

The  $N$  successive deterministic evaluations needed for the regression method are the most expensive part of the gPCE implementation, especially for large scale FE models, large number of uncertain parameters, presence of nonlinearities and number of iterations required for computing the structural response. To overcome this problem, the ROMs are incorporated in the regression method. In fact, the deterministic responses  $\{y(\xi^{(n)}), n = 1, \dots, N\}$  are projected on the enriched reduction basis.

## 2.2. First-level metamodel

In order to build the first robust metamodel, the gPCE method is combined with a first-level ROM. Here, we propose to compute the deterministic responses  $\{y(\xi^{(n)}), n = 1, \dots, N\}$ , needed for the regression method, using an enriched basis (EB).

Practically, in stochastic case with localized nonlinearities, using standard truncated normal modes basis  $\mathbf{T} = \boldsymbol{\phi}_r$  may not allow the required level of accuracy to be reached even if more eigenvectors are computed. The  $\boldsymbol{\phi}_r$  basis does not contain any information about uncertainties and nonlinearities since it is relative to the associated deterministic linear system.



Therefore, adding a complementary sub-basis  $\Delta\mathbf{T}$  to enrich  $\boldsymbol{\phi}_r$  is necessary. The obtained EB is thus of the form

$$\mathbf{T} = [\boldsymbol{\phi}_r \quad \vdots \quad \Delta\mathbf{T}] \quad (7)$$

The complementary sub-basis  $\Delta\mathbf{T}$  contains properly selected static residual vectors according to the type of enrichment.

In order to account for localized nonlinearities effects, a complementary basis must be created (Bouazizi et al. 2006) according to the following form

$$(\Delta\mathbf{T}_{NL})_i = K_0^{-1}F_i, i = 1, \dots, m \quad (8)$$

where  $K_0$  is the deterministic stiffness matrix and  $F_i$  is the residual force vectors containing unit values in nonlinear degrees of freedom and zeros otherwise,  $m$  is the total number of nonlinear dofs.

Enriching the basis by taking into account stochastic effects (Guedri et al. 2006) requires computing the residual vectors as

$$\Delta\mathbf{T}_S = R\mathbf{F}_S \quad (9)$$

where

$$R = K_0^{-1} - \boldsymbol{\phi}_r \Lambda_r^{-1} \boldsymbol{\phi}_r^T \quad (10)$$

is the static residual flexibility matrix and  $\mathbf{F}_S$  is a force basis including stochastic effects.  $\Lambda_r$  is the spectral one (containing only the first  $n_r$  retained eigenvalues). The force basis is generated depending on the stochastic zones of the mass and stiffness matrices. In fact, for each stochastic zone  $j$ , the force sub-basis  $F_S^j$  is of the form

$$F_S^j = [F_K^j \quad \vdots \quad F_M^j] = [\sum_{n=1}^N K_n^j(\xi) \boldsymbol{\phi}_r \quad \vdots \quad \sum_{n=1}^N M_n^j(\xi) \boldsymbol{\phi}_r \Lambda_r] \quad (11)$$

where  $K_i^j$  and  $M_i^j$  are the stochastic stiffness and mass matrices taking into account the uncertainties in each stochastic zone  $j$ . The different sub-bases are then grouped to form the force basis  $F_S$  and the singular value decomposition (SVD) is needed to ensure its linear independence. The sub-basis  $\Delta T_S$  is thereafter obtained using Eq. (9) and added to the standard one.

The ROM basis can also be enriched by considering the external loading effects. Thus, an additional sub-basis must be computed as

$$\Delta T_E = R F_E \quad (12)$$

where  $F_E$  are successive unit static loadings imposed on internal excited dofs.

Once complementary sub-bases  $\Delta T_{NL}$ ,  $\Delta T_S$  and  $\Delta T_E$  have been calculated, the EB takes the following form

$$\mathbf{T} = [\boldsymbol{\phi}_r \quad : \quad \Delta T_{NL} \quad : \quad \Delta T_S \quad : \quad \Delta T_E] \quad (13)$$

It should be noted that it is necessary to normalize  $\Delta T_{NL}$ ,  $\Delta T_S$  and  $\Delta T_E$  similarly to the standard basis  $\boldsymbol{\phi}_r$  to ensure the orthogonality of the different vectors. Furthermore, a singular value decomposition (SVD) must also be carried out to ensure linear independence of the vectors forming each complementary sub-basis and also carried out on  $\mathbf{T}$  to ensure the linear independence of the sub-bases and thus the well-conditioning of  $\mathbf{T}$ . Consequently, the obtained EB contains  $n_r + n_e$  columns, where  $n_r$  and  $n_e$  represent respectively the numbers of retained normal modes and enriching static residual vectors.

### 2.3. Second-level metamodel

The second robust metamodel extends the reduction to a second-level ROM based on the CB-CMS. The  $N$  deterministic responses  $\{y(\xi^{(n)}), n = 1, \dots, N\}$ , needed for the gPCE regression method are thus computed using an enriched Craig-Bampton transformation (ECBT).

In fact, dividing the complete structure into several components is useful when we deal with large scale FE models including uncertainties and localized nonlinearities. It permits to apply the reduction and enrichment methods to each component with uncertain parameters and/or localized nonlinearities independently of the others. Moreover, it permits to exploit component periodicity in the case of periodic structures as shown in Section 3.3.

In the deterministic linear case, the ROM is obtained using standard CB-CMS. The CBT is defined, for a component  $k$ , as

$$\mathbf{y}^k = \begin{Bmatrix} \mathbf{y}_j \\ \mathbf{y}_i \end{Bmatrix}^k = \begin{bmatrix} I_{jj} & 0 \\ \boldsymbol{\psi}_{ij} & \boldsymbol{\varphi}_i \end{bmatrix}^k \begin{Bmatrix} \mathbf{y}_j \\ \mathbf{q}_i \end{Bmatrix}^k = \mathbf{T}_{CB}^k \mathbf{q}^k \quad (14)$$

where  $\mathbf{y}_i^k$  are the coordinates of the nodes in the interior of the component reduced to modal coordinates  $\mathbf{q}_i^k$ ,  $\mathbf{y}_j^k$  are the coordinates of the nodes located at the interface between components,  $\boldsymbol{\psi}_{ij}^k = -(\mathbf{K}_{ii}^k)^{-1} \mathbf{K}_{ij}^k$  is the static sub-basis containing constrained modes,  $I_{jj}$  is the identity matrix, and  $\boldsymbol{\varphi}_i^k$  is the truncated basis containing the first  $n_r$  normal modes of the corresponding component. However, standard CBT may entail computing even all normal modes to achieve accurate results, which may be not affordable computationally.

In the case of stochastic structural response including localized nonlinearities, enrichment of standard CBT  $\mathbf{T}_{CB}$  is done similarly to the first-level ROM described in Section 2.2.

In fact, for each component  $k$ , the static residual flexibility matrix is of the form

$$\mathbf{R} = \mathbf{K}_{ii}^{-1} - \begin{bmatrix} 0 \\ \boldsymbol{\varphi}_i \end{bmatrix} \Lambda^{-1} [0 \quad \boldsymbol{\varphi}_i^T] \quad (15)$$

and for each stochastic zone  $j$  in  $k$ , the force sub-basis  $\mathbf{F}_S^j$  is expressed as

$$\mathbf{F}_S^j = [\mathbf{F}_K^j \quad \vdots \quad \mathbf{F}_M^j] = \left[ \sum_{n=1}^N (\mathbf{K}_{ii})_n^j(\xi) \begin{bmatrix} 0 \\ \boldsymbol{\varphi}_i \end{bmatrix} \quad \vdots \quad \sum_{n=1}^N (\mathbf{M}_{ii})_n^j(\xi) \begin{bmatrix} 0 \\ \boldsymbol{\varphi}_i \end{bmatrix} \Lambda \right] \quad (16)$$

The obtained ECBT  $\mathbf{T}_{ECB}$ , for each component  $k$ , is thus of the form

$$\begin{aligned}\mathbf{T}_{ECB}^k &= [\mathbf{T}_{CB} \quad \vdots \quad \Delta\mathbf{T}_{NL} \quad \vdots \quad \Delta\mathbf{T}_S \quad \vdots \quad \Delta\mathbf{T}_E]^k \\ &= \begin{bmatrix} I_{jj} & 0 & \vdots & 0 & \vdots & 0 & \vdots & 0 \\ \psi_{ij} & \varphi_i & \vdots & \Delta\mathbf{T}_{NL} & \vdots & \Delta\mathbf{T}_S & \vdots & \Delta\mathbf{T}_E \end{bmatrix}^k\end{aligned}\quad (17)$$

Assembling the ECBT  $\mathbf{T}_{ECB}^k$  allows forming a global transformation matrix  $\mathbf{T} = \mathbf{T}_{ECB}$  which contains  $n_j + n_r + n_e$  columns, where  $n_j$ ,  $n_r$  and  $n_e$  represent respectively the number of the junction dofs, the number of the retained normal modes and the number of the enriching static residual vectors.

## 2.4. Nonlinear time analysis

Projection of the time response on a reduction basis is made using the variable transform  $\mathbf{y}(t) = \mathbf{T}\mathbf{q}(t)$  to modal coordinates. Hence, the equation of motion (1) becomes

$$\begin{cases} M_r \ddot{\mathbf{q}}(t) + B_r \dot{\mathbf{q}}(t) + \mathbf{T}^T f_{int}(\mathbf{T}\mathbf{q}) = \mathbf{T}^T f_{ext} \\ q_0 = \mathbf{T}^+ y_0 \\ \dot{q}_0 = \mathbf{T}^+ \dot{y}_0 \\ \ddot{q}_0 = M_r^{-1}(\mathbf{T}^T f_{ext}(t_0) - B_r \dot{q}_0 - \mathbf{T}^T f_{int}(\mathbf{T}q_0)) \end{cases}\quad (18)$$

where the index  $r$  is relative to the reduced terms,  $\mathbf{T}^+$  the pseudo-inverse of  $\mathbf{T}$ ,  $M_r = \mathbf{T}^T \mathbf{M} \mathbf{T}$  and  $B_r = \mathbf{T}^T \mathbf{B} \mathbf{T}$ . In this case, the internal forces vector is expressed as

$$f_{int}(\mathbf{T}\mathbf{q}) = (\mathbf{K} + f_{NL}(\mathbf{T}\mathbf{q}))\mathbf{T}\mathbf{q}\quad (19)$$

The time solution of the Eq. (18) can be approximated using the Newmark nonlinear time integration scheme ((Newmark, 1959), (Gérardin and Rixen 1997), (Krenh 2009), (Lulf et al. 2013), (Wenneker and Tiso, 2014)). At time  $t_{n+1}$ , this equation is expressed as follows

$$M_r \ddot{\mathbf{q}}_{n+1} + B_r \dot{\mathbf{q}}_{n+1} + \mathbf{T}^T f_{int}(\mathbf{T}\mathbf{q}_{n+1}) - \mathbf{T}^T f_{ext}(t_{n+1}) = \mathbf{r}_{n+1}\quad (20)$$

where  $\mathbf{r}_{n+1}$  is the generalized residual force vector which must be minimized using an iterative Newton-Raphson algorithm. For the iteration  $i$ , the incremental solution  $\Delta\mathbf{q}_{n+1}^i$  is calculated by

$$\Delta\mathbf{q}_{n+1}^i = -(\tilde{\mathbf{K}}_r^i)^{-1} \mathbf{r}_{n+1}^i\quad (21)$$

where  $\tilde{K}_r^i$  is the instantaneous stiffness matrix (Jacobian of the system) defined by

$$\tilde{K}_r^i = K_T^i + \frac{\gamma}{\beta h} B_r + \frac{1}{\beta h^2} M_r \quad (22)$$

function of the tangent stiffness matrix

$$K_T^i = \mathbf{T}^T \left( \left[ \frac{\partial f_{int}(\mathbf{T}q)}{\partial (\mathbf{T}q)} \right]_{\mathbf{T}q_{n+1}^i} \right) \mathbf{T} \quad (23)$$

In order to illustrate the main features of the proposed metamodels and to evaluate their robustness against uncertainties and localized nonlinearities, two numerical examples are presented in Section 3.

### 3. NUMERICAL APPLICATIONS

#### 3.1. Evaluation criteria

To evaluate the efficiency of the proposed metamodels, two main criteria must be satisfied: the reduction of computational cost with respect to the reference full model and the accuracy of the approximate responses.

The first criterion is verified by comparing the CPU time required by each method. For the second criterion, a set of statistic time indicators must be calculated to assess response accuracy in terms of amplitude and periodicity errors. These indicators are function of statistical moments similar to the temporal moments  $\mathcal{M}_i$  used in ((Smallwood, 1994), (Hemez and Doebling, 2003)) in the case of transient time responses and defined by

$$\mathcal{M}_i = \int_{-\infty}^{+\infty} (t - t_s)^i y(t)^2 dt \quad (24)$$

where  $y(t)$  is the transient time response,  $i$  the order of the moment and  $t_s$  the temporal shift.

To take into account discrete data and overcome the convergence problem of integral (24) encountered when stationary time responses are considered, the  $i^{th}$  adapted moment  $m_i$  is computed using a discrete sum which is truncated at time  $t_f$ :

$$m_i = \sum_{t=0}^{t_f} t^i y(t)^2 \quad (25)$$

where the interval  $[0, t_f]$  contains a finite number of periods of the stationary response  $y(t)$ .

To verify the accuracy of the responses in term of amplitude, a first indicator  $I_1$  is defined by:

$$I_1 = m_0 \quad (26)$$

And in term of periodicity, two indicators  $I_2$  and  $I_3$  are defined by:

$$I_2 = m_1/m_0 \quad (27)$$

$$I_3 = m_2/m_0 - (m_1/m_0)^2 \quad (28)$$

## 3.2. First-level metamodel example

### 3.2.1. Proposed structure and process

The performance of the first-level metamodel is evaluated by computing the time response of the 2D frame structure shown in Figure 1. The FE model of the frame includes 160 beam elements with three dofs per node ( $u_x, v_y, \theta_z$ ) for a total of 474 dofs. The mechanical and geometrical properties of the frame structure are: width  $b = 0.03 \text{ m}$ , thickness  $h_0 = 0.05 \text{ m}$ , length  $L = 1.5 \text{ m}$ , Young Modulus  $E_0 = 2.1 \times 10^{11} \text{ Pa}$ , density  $\rho_0 = 7800 \text{ kg.m}^{-3}$  and Poisson ratio  $\nu = 0.3$ . The damping of the structure is supposed to be proportional with a modal damping  $\eta = 0.05$ .

Two localized nonlinear Duffing springs of stiffness  $k_{NL} = 10^{16} \text{ N.m}^{-3}$  are linked to the frame structure as shown in Figure 1. The structure is submitted to two forces  $F_1(N) = 10^3 \times \cos(\omega_5 t)$

and  $F_2(N) = 10^4 \times \cos(\omega_5 t)$ , applied at the dofs  $P_{f1}$  and  $P_{f2}$ , exciting its fifth normal mode ( $\omega_5 = 1435.9 \text{ rad.s}^{-1}$ ). Note that the excitation frequency is arbitrarily chosen.

The Young modulus  $E$  and the density  $\rho$  of respectively the left and the right vertical beams of the frame structure and the thickness  $h$  of its horizontal beam section are considered to be the three stochastic parameters such as

$$\begin{aligned} E &= E_0(1 + \sigma_E \xi_E) \\ \rho &= \rho_0(1 + \sigma_\rho \xi_\rho) \\ h &= h_0(1 + \sigma_h \xi_h) \end{aligned} \quad (29)$$

where  $\xi_E$ ,  $\xi_\rho$  and  $\xi_h$  are random variables of respectively lognormal, lognormal and exponential probability distributions; the considered dispersion values are:  $\sigma_E = \sigma_\rho = 20\%$  and  $\sigma_h = 10\%$ . The time responses computation is done in the time interval  $[0 - 0.2 \text{ s}]$ , divided into steps of  $1 \times 10^{-4} \text{ s}$ , in which the stationary regime is already attained.

The obtained results are discussed with respect to the responses considered as reference, computed using the LHS method for 1000 samples of random variables. The comparison concerns the LHS method implemented on the full FE model (noted LHS-REF) and the reduced model (LHS-MB and LHS-EB using respectively modal and enriched basis) model, and the gPCE regression method on the full (gPC-REF) and the reduced (gPC-EB) models. The results discussed below correspond to two arbitrarily chosen observation dofs  $P_{o1}$  and  $P_{o2}$ .

### 3.2.2. Results and discussion

As mentioned in Section 2.2, in the first-level reduction order model, denoted as EB,  $n_r$  retained normal modes and  $n_e$  enriching static residual vectors are included as the  $(n_r + n_e)$  dofs in the reduced FE model. The number  $n_r$  of retained normal modes depends on the frequency range of interest and its modal density. Generally,  $n_r$  covers 2, up to 3, times this frequency

range. The number  $n_e$  of static residual vectors depends on the number of: uncertainty zones, localized nonlinearities and external excitations. This number is known when applying the SVD technique.

In this example, the EB contains  $n_r = 20$  retained normal modes and  $n_e = 37$  enriching static residual vectors. At first, 44 static residual vectors are computed which include: 40 uncertainty vectors, 2 localized nonlinearities vectors and 2 external excitations vectors. When applying the SVD technique, the sub-basis of 44 residual vectors is reduced to 37 vectors. Hence, the full model of 474 dofs is transformed to a reduced model of  $n_r + n_e = 57$  dofs leading to a reduction ratio of 88 %. Note that refining the initial FE model induces a significant increase in the full model size with a slight increase of the reduced one. This can lead to more important reduction ratio.

The obtained results of different models are compared in terms of accuracy and time consuming by means of the time indicators  $I_1$ ,  $I_2$  and  $I_3$  and the CPU computation time (Table 1). In fact, Table 1 recalls the size of the problems to be solved and the size of the ED (number of samples for LHS method and regression points for gPCE) and gives the values of the associated time indicators and the CPU computational time values.

The effect of uncertainties is shown using the MAC (Modal Assurance Criterion) matrix (Figure 2) which compares the normal modes of the deterministic model to the means of the modes of the stochastic model computed with correspondence to each random variable using the LHS-REF reference model. Indeed, if the  $MAC_{ij} = 1$ , the eigenmodes  $\phi_i$  and  $\phi_j$  are consistent. If  $MAC_{ij} = 0$ , no correlation between these modes occurs. This criterion decreases, in fact, when the modal perturbation level resulting from uncertainties increases and thus modal correlation is disturbed. For more clarity, the (1-MAC) matrix is represented. Figure 3 shows also the



stochastic effect through the superposition of the deterministic responses and the mean of the stochastic responses.

The levels of uncertainties and nonlinearities are designed to be high in order to show the robustness of the enriched basis (EB) compared to the modal basis (MB). This is illustrated through Figures 4 and 5 and Table 1. Figures 4 and 5 compare the means of the responses (displacements and phase diagrams) computed using these bases of same size (57 vectors) to the mean of the reference response obtained using the full FE model.

To judge the EB efficiency in term of accuracy and time consuming, the time indicators and the CPU time are listed in Table 1. The proposed reduction method allows, in fact, a reduction of 46 % of the computational time with small errors on accuracy (Table 1; line 3).

Experiments design (ED) to build second, fourth and sixth order gPCE approximations, respectively, utilized 17, 57 and 171 combinations of random variables chosen accordingly to Eqs. (5-6) among, respectively, 27, 125 and 343 Hermite polynomial roots combinations  $((p + 1)^d$ , where  $d = 3$  is the number of random variables) and then transformed with respect to the probability distributions using iso-probabilistic transformations.

Figures 6 and 7 compare the means of stochastic displacements and phase diagrams obtained by second and sixth order gPCE method implemented on the full FE model at the two chosen observation points. It can be seen that increasing the order of the approximation allows improving accuracy but also entails a higher computational cost (see Table 1). Furthermore, gPCE approximations become less accurate at the dofs for which response is more sensitive to nonlinearity.

The comparison between the means of stochastic displacements and phase diagrams obtained by sixth order gPCE method implemented on the full FE model and ROM and those

computed using the full FE model is shown through Figures 8 and 9 and the time indicator values listed in Table 1, which correspond to the means of response moments computed for all dofs.

To conclude, the first-level metamodel can replace the reference full model without a significant loss of accuracy. It leads in fact to 90 % of computational time gain with only 0.6 % of accuracy error for a sixth order gPCE approximation, in spite of the presence of significantly localized sources of nonlinearity that result in a globally nonlinear behavior of the frame. As suggested in literature (see introduction), using variants of gPCE method is better than increasing the order of the gPCE as the latter increases the computational cost of the approximation.

**Table 1.** Model size, associated time indicators and CPU time

Methods		ED size	Model (dofs)	Time indicators (error %)			CPU (%)
				$I_1$	$I_2$	$I_3$	
LHS	REF	1000	474	-	-	-	100
	MB	1000	57	2.60	0.20	0.30	49.2
	EB	1000	57	0.07	0.00	0.00	53.7
Order 2	REF	17	474	20.20	2.15	2.13	1.8
	EB	17	57	20.27	2.15	2.13	0.9
gPC Order 4	REF	57	474	6.80	1.26	1.52	6.0
	EB	57	57	6.87	1.26	1.52	3.2
Order 6	REF	171	474	0.13	0.52	0.61	18.3
	EB	171	57	0.07	0.52	0.61	9.8

Combining gPCE approximation with ROM allowed reducing computational cost by 50% with respect to the case of a sixth order gPCE implemented on the full FE model (i.e. from 18.3%

to 9.8% of the CPU time required by LHS for the full FE model). Such a gain should become more significant for systems including larger FE models and more uncertain parameters.

### 3.3. Second-level metamodel example

#### 3.3.1. Proposed structure and process

Micro/Nano-electromechanical systems (M/NEMS) are microscopic devices operating with a power source and with applications in a variety of fields such as biotechnology, biomedicine, aerospace, automotive, robotics and manufacturing. MEMS arrays can be formed by several coupled resonators for specific applications such as multi-mass or gas sensing (Kacem et al., 2010). Designing M/NEMS arrays can present some limitations like coupling between components, dispersion and complexity control especially in presence of uncertainties and localized or distributed nonlinearities (Liu et al., 2007). The concept of MEMS model reduction remains an important challenge in the scientific community and many authors deal with the development of ROMs for MEMS design ((Nayfeh et al., 2005), (Lazarus et al., 2012)). Here, we propose to apply the second-level metamodel to evaluate the time response of a micro-system containing uncertain parameters and localized nonlinearities. The system, Figure 10, is comprised of twenty identical micro-beams submitted to transversal vibration. Each micro-beam is discretized into 20 elements with two dofs per node  $(v_y, \theta_z)$  for a total of 800 dofs. The micro-beams are of rectangular section with  $b = 3 \mu m$  and  $h = 1 \mu m$ , length  $L_b = 50 \mu m$ , Young modulus  $E_0 = 169 GPa$  and density  $\rho_0 = 2330 kg.m^{-3}$ . Each beam is submitted to a localized excitation force  $P_f(N) = 10^{-6} \times \cos(2\pi f_1 t)$  according to the  $v_y$  dof ( $Y$  direction), where  $f_1 = 565.53 \times 10^3 Hz$  is the first eigenfrequency which has been chosen in order to avoid parasitic capacitances at higher frequencies (Kacem et al. 2015). The twenty micro-beams are coupled using twenty localized dampers such as  $c = 10^{-5} N.s.m^{-1}$ , twenty linear springs

$k_0 = 10N.m^{-1}$  and Duffing nonlinear springs  $k_{NL} = 10^{14}N.m^{-3}$ . Several observation dofs  $P_{oj}$  ( $j = 1, 2, \dots$ ) are considered to evaluate the efficiency of the proposed metamodel.

The time responses evaluation is done in the time interval  $[0 - 5 \times 10^{-5} \text{ s}]$ , divided into steps of  $10^{-8} \text{ s}$ , enough to reach a stationary condition.

To apply the CB-CMS method, the complete structure is divided into 20 components. Since the structure is periodic, each set of coupling elements (localized damper, linear and nonlinear springs) and a micro-beam is considered as a component (Figure 10). The first, the third and the fifteenth components are considered as three stochastic zones in which the Young modulus of the micro-beam and the linear coupling stiffness are supposed to be the uncertain parameters such as

$$\begin{aligned} E_i &= E_0(1 + \sigma_{E_i}\xi_{E_i}) \\ k_i &= k_0(1 + \sigma_{k_i}\xi_{k_i}) \end{aligned} \quad (30)$$

where  $i = 1, 3, 15$ ,  $\xi_{E_i}$  and  $\xi_{k_i}$  are two types of random variables of respectively uniform and lognormal probability distributions and  $\sigma_{E_i} = \sigma_{k_i} = 10\%$  are the considered dispersions.

The process followed in this configuration, in order to evaluate the efficiency of the second proposed metamodel, is the same as the first configuration, with replacing the EB by the ECBT matrix.

### 3.3.2. Results and discussion

The effect of the uncertainties is shown using the MAC matrix for the linear structure, Figure 11. Differently from the example of Section 3.2, Figure 2, the (1-MAC) matrix is here more diagonal dominated since the effect of uncertainties is lower.

The ECBT matrix contains  $n_j = 38$  junctions dofs,  $n_r = 1$  retained normal mode per component and  $n_e = 6$  enriching static residual vectors corresponding to uncertainties and

localized nonlinearities for 3 components;  $n_e = 17$  enriching static residual vectors corresponding to nonlinearities for 17 components and  $n_e = 1$  enriching static residual vector corresponding to external excitation localized on one component. Consequently, the full model of 800 dofs is transformed to a reduced model of 82 dofs leading to a reduction ratio of 90 %. Here also, if refining the initial FE model is required, this refinement induces a significant increase in the full model size with a slight increase of the reduced one. More important reduction ratio could be then obtained.

As mentioned above, the choice of the gPCE order depends on the level of uncertainty, the level of localized nonlinearity and the required accuracy. For this example, which is less affected by uncertainties and nonlinearities than the 2D frame example, a second order gPCE is sufficient to approximate accurately the time response. In this case, the ED is of size 73 random variables combinations chosen accordingly to Eqs. (5-6) among 729 Hermite polynomial roots combinations ( $(p + 1)^d = 3^6 = 729$ , where  $d = 6$  derives from having defined two random variables for each component 1, 3 and 15) and then transformed with respect to the probability distributions. Hence, the number of analyses required for building the second order gPCE approximation decreased by 92.7% with respect to LHS implemented on the full FE model (only 73 analyses vs. 1000 analyses).

Similar to the first-level metamodel efficiency evaluation, a comparison of the obtained results of different methods is illustrated, also in terms of accuracy and time consuming by means of the CPU computation time and the time indicators  $I_1$ ,  $I_2$  and  $I_3$  (see Table 2).

In this case, the responses are presented in terms of velocities in order to illustrate the effect of the nonlinearities. Figure 12 illustrates the comparison between the means of stochastic velocities obtained by the ECB method and the LHS reference method.

As illustrated in Table 2 and Figure 12, implementing the LHS method on the ECBT (LHS-ECBT) compared to its implementation on the full FE model (LHS-REF) results in only 2.5% error but with a 55% reduction of CPU time.

**Table 2.** Model size, associated time indicators and CPU time

Methods		ED size	Model (dofs)	Time indicators (error %)			CPU (%)	
				$I_1$	$I_2$	$I_3$		
LHS	REF	1000	800	-	-	-	100	
	ECBT	1000	82	2.50	0.07	0.14	45.1	
gPC	Order 2	REF	73	800	0.00	0.07	0.14	6.5
	ECBT	73	82	2.50	0.20	0.41	2.8	

Furthermore, Figure 13 compares the LHS approximation built on the full FE model and the second order gPCE approximation built using the full model or the ECBT model on only 82 dofs. The approximate model again yield only 2.5% error but computational cost was reduced by 97.1% with respect to LHS applied to the full model. The gPCE approximation built on the full model is computationally efficient as it requires only 6.5% of the CPU required by the full LHS model.

The second example fully demonstrates how exploiting structure periodicity to simplify the implementation of the Craig-Bampton method.

To recapitulate, six metamodels were implemented in this work:

- The LHS method applied on the full model : LHS-REF;
- The gPCE method applied on the full model : gPC-REF;
- The LHS method applied on the first-level ROM : LHS-EB;

- The gPCE method applied on the first-level ROM : gPC-EB;
- The LHS method applied on the second-level ROM : LHS-ECBT;
- The gPCE method applied on the second-level ROM : gPC-ECBT.

They can be summarized through the following scheme, Figure 14:

#### 4. CONCLUDING REMARKS

With the aim of quantifying and propagating parametric uncertainties in models containing localized nonlinearities, two robust metamodels were proposed, in this paper. The first metamodel combines the gPCE uncertainty propagation method and a first-level ROM based on the enrichment of the Ritz basis using residual vectors which take into account both uncertainties and localized nonlinearities effects. The second metamodel, which is adapted to the Craig-Bampton method in the context of the CMS, allows the enrichment of the reduction bases of some components containing uncertainties and/or localized nonlinearities independently of the others. The proposed metamodels were evaluated in terms of robustness and efficiency by solving two structural dynamics problems of a 2D frame and a periodic micro-beams structure. For that purpose, a detailed comparison between six metamodels including Latin Hypercube Sampling, first and second level condensation applied on the FE model including all dofs or on a reduced FE model was carried out. Numerical results proved that the present approach allows to approximate stochastic/nonlinear structural behavior at a reasonably low computational cost and without losing accuracy with respect to the reference model using the LHS uncertainty propagation method applied to the full FE model of the investigated structure.

The most frequently encountered issue of the gPCE method is the choice of the appropriate order of the expansion according to the complexity of the problem, the number of the



uncertain parameters in order to insure the convergence of the solution to the real structure behavior. In the case of large scale FE models and great number of uncertain parameters, the cost of the gPCE method becomes prohibitive. Therefore, it is interesting to apply the proposed metamodels combining the gPCE with ROMs.

## REFERENCES

- Afonso S.M.B., Motta R.S. (2013), "Structural optimization under uncertainties considering reduced-order modeling", *10<sup>th</sup> World Congress on Structural and Multidisciplinary Optimization*, May 19-24, Orlando, Florida, USA.
- Balmès E. (1996a), "Parametric families of reduced finite element models: Theory and applications", *Mechanical Systems and Signal Processing*, Vol. 10 No. 4, pp. 381-394.
- Balmès E. (1996b), "Optimal Ritz Vectors for Component Mode Synthesis Using the Singular Value Decomposition", *AIAA Journal*, Vol. 34 No. 6.
- Ben Souf M.A., Ichchou M., Bareille O., Bouhaddi N., Haddar M. (2015), "Dynamics of random coupled structures through the wave finite element method", *Engineering Computations: International Journal for Computer-Aided Engineering and Software*, Vol. 32 No. 7, 2015, pp. 2020-2045.
- Berveiller M., Sudret B., Lemaire M. (2006), "Stochastic finite element: a non-intrusive approach by regression", *European Journal of Computational Mechanics*, Vol. 15 No. 1-3, pp. 81-92.
- Blanchard E., Sandu A., Sandu C. (2009), "Parameter estimation for mechanical systems via an explicit representation of uncertainty", *Engineering Computations: International Journal for Computer-Aided Engineering and Software*, Vol. 26 No. 5, pp. 541-569.
- Blatman G., Sudret B. (2010), "An adaptive algorithm to build up sparse polynomial chaos expansions for stochastic finite element analysis", *Probabilistic Engineering Mechanics*, Vol. 25, pp. 183-197.
- Bouazizi M.L., Guedri M., Bouhaddi N. (2006), "Robust component modal synthesis method adapted to the survey of the dynamic behavior of structures with localized nonlinearities", *Mechanical Systems and Signal Processing*, Vol. 20, pp. 131-157.
- Bouazzouni A., Lallement G., Cogan S. (1997), "Selecting a Ritz basis for the reanalysis of the frequency response functions of modified structures", *Journal of Sound and Vibration*, Vol. 199 No. 2, pp. 309-322.
- Chiang W.-L., Dong W.-M., Wong F.S. (1987), "Dynamic response of structures with uncertain parameters: A comparative study of probabilistic and fuzzy sets models", *Probabilistic Engineering Mechanics*, Vol. 2 No. 2, pp. 82-91.
- Chouvion B., Sarrouy E. (2016), "Development of error criteria for adaptive multi-element polynomial chaos approaches", *Mechanical Systems and Signal Processing*, Vol. 66-67, pp. 201-222.

- Craig Jr.R.R., Bampton M.C.C. (1968), "Coupling of substructures for dynamic analyses", *AIAA Journal*, Vol. 6 No. 7, pp. 1303-1319.
- De Lima A.M.G., Da Silva A.R., Rade D.A., Bouhaddi N. (2010), "Component mode synthesis combining robust enriched Ritz approach for viscoelastically damped structures", *Engineering Structures*, Vol. 32, pp. 1479-1488.
- Dell'Elce L., Kerschen G. (2015), "Probabilistic Assessment of Lifetime of Low-Earth-Orbit Spacecraft: Uncertainty Propagation and Sensitivity Analysis", *Journal of Guidance, Control, and Dynamics*, Vol. 38 No. 5, pp. 886-899.
- Deman G., Konakli K., Sudret B., Kerrou J., Perrochet P., Benabderrahmane H. (2016), "Using sparse polynomial chaos expansions for the global sensitivity analysis of groundwater lifetime expectancy in a multi-layered hydrogeological model", *Reliability Engineering and System Safety*, Vol. 147, pp. 156-169.
- Dubreuil S., Berveiller M., Petitjean F., Salaün M. (2014), "Construction of bootstrap confidence intervals on sensitivity indices computed by polynomial chaos expansion", *Reliability Engineering & System Safety*, Vol. 121, pp. 263-275.
- Gaurav, Wojtkiewicz S.F., Johnson E.A. (2011), "Efficient uncertainty quantification of dynamical systems with local nonlinearities and uncertainties", *Probabilistic Engineering Mechanics*, Vol. 26, pp. 561-569.
- Gérardin M, Rixen D. (1997), "*Mechanical Vibrations: Theory and Application to Structural Dynamics*", second edition, John Wiley & Sons.
- Gerritsma M., Van der Steen J.-B., Vos P., Karniadakis G. (2010), "Time-dependent generalized polynomial chaos". *Journal of Computational Physics*, Vol. 229, pp. 8333-8363.
- Ghanem R., Spanos P. (1991), "*Stochastic finite elements-a spectral approach*", Springer, Berlin.
- Guedri M., Bouhaddi N., Majed R. (2006), "Reduction of the stochastic finite element models using a robust dynamic condensation method", *Journal of Sound and Vibration*, Vol. 297, pp. 123-45.
- Guedri M., Weisser T., Bouhaddi N. (2010), "Reanalysis of nonlinear structures by a reduction method of combined approximations", *Proceedings of the 10<sup>th</sup> International Conference on Computational Structures Technology (CST 2010)*, pp. 312.
- Guerine A., El Hami A., Walha L., Fakhfakh T., Haddar M. (2016), "A polynomial chaos method for the analysis of the dynamic behavior of uncertain gear friction system". *European Journal of Mechanics-A/Solid*, Vol 59, pp. 76-84.
- Hayes R., Marques S.P. (2015), "Prediction of limit cycle oscillations under uncertainty using a Harmonic Balance method". *Computer and Structures*, Vol. 148, pp. 1-13.
- Helton J.C., Davis F.J. (2003), "Latin hypercube sampling and the propagation of uncertainty in analyses of complex systems", *Reliability Engineering & System Safety*, Vol. 81, pp. 23-69.
- Hemez F.M., Doebling S.W. (2003), "From shock response spectrum to temporal moments and vice-versa", *International Modal Analysis Conference (IMAC-XXI)*, February 3-6, Kissimmee, Florida.
- Hinke L., Dohnal F., Mace B.R., Waters T.P., Ferguson N.S. (2009), "Component mode synthesis as a framework for uncertainty analysis", *Journal of Sound and Vibration*, Vol. 324, pp. 161-178.

- Jacquelin E., Adhikari S., Sinou J.-J., Friswell M.I. (2015), “Polynomial chaos expansion in structural dynamics: Accelerating the convergence of the first two statistical moment sequences”, *Journal of Sound and Vibration*, Vol. 356, pp. 144-154.
- Jacquelin E., Friswell M.I., Adhikari S., Dessombz O., Sinou J.-J. (2016), “Polynomial chaos expansion with random and fuzzy variables”, *Mechanical Systems and Signal Processing*, Vol. 75, pp. 41-56.
- Kacem N., Arcamone J., Perez-Murano F., Hentz S. (2010), “Dynamic range enhancement of nonlinear nanomechanical resonant cantilevers for high sensitive NEMS gas/mass sensors applications”, *Journal of Micromechanics and Microengineering*, Vol. 20, No. 4, 045023.
- Kacem N., Baguet S., Duraffourg L., Jourdan G., Dufour R., Hentz S. (2015), “Overcoming limitations of nanomechanical resonators with simultaneous resonances”, *Applied Physics Letters*, Vol. 107 No. 7, pp. 073-105.
- Kerschen G., Golinval J.C., Vakakis A.F., Bergman L.A. (2005), “The Method of Proper Orthogonal Decomposition for Dynamical Characterization and Order Reduction of Mechanical Systems: An Overview”, *Nonlinear Dynamics*, Vol. 41, pp. 147-169.
- Kirsh U. (2000), “Combined approximations - a general reanalysis approach for structural optimization”, *Structural and Multidisciplinary Optimization*, Vol. 20, pp. 97-106.
- Krenk S. (2009), “*Non-linear Modeling and Analysis of Solids and Structures*”, Cambridge University Press.
- Kuether R.J., Brake M.R., Allen M.S. (2014), “Evaluating Convergence of Reduced Order Models Using Nonlinear Normal Modes”, *Model Validation and Uncertainty Quantification*, Vol. 3, Conference Proceedings of the Society for Experimental Mechanics Series, pp. 287-300.
- Lazarus A., Thomas O., Deü J.-F. (2012), “Finite elements reduced order models for nonlinear vibrations of piezoelectric layered beams with applications to NEMS”, *Finite Elements in Analysis and Design*, Vol. 49 No. 1, pp. 35-51.
- Liang Y., Lee H., Lim S., Lin W., Lee K., Wu C. (2002), “Proper orthogonal decomposition and its applications—part I: Theory”, *Journal of Sound and Vibration*, Vol. 252 No. 3, pp. 527-544.
- Liu M., Maute K., Frangopol D.M. (2007), “Multi-objective design optimization of electrostatically actuated microbeam resonators with and without parameter uncertainty”, *Reliability Engineering & System Safety*, Vol. 92 No. 10, pp. 1333-1343.
- Lulf F.A., Tran D.-M., Ohayon R. (2013), “Reduced bases for nonlinear structural dynamic systems: A comparative study”, *Journal of Sound and Vibration*, Vol. 332 No. 3, pp. 897-921.
- Masson G., Ait Brik B., Cogan S., Bouhaddi N. (2006), “Component mode synthesis CMS based on an enriched Ritz approach for efficient structural optimization”, *Journal of Sound and Vibration*, Vol. 296 No. 4-5, pp. 845-860.
- Maute K., Weickum G., Eldred M. (2009), “A reduced-order stochastic finite element approach for design optimization under uncertainty”, *Structural Safety*, Vol. 31, pp. 450-459.
- Mohammadali M., Ahmadian H. (2014), “Efficient model order reduction for dynamic systems with local nonlinearities”, *Journal of Sound and Vibration*, Vol. 333, pp. 1754-1766.

- Motta R.S., Afonso S.M.B., Lyra P.B., Willmersdorf R.B. (2015), "Development of a computational efficient tool for robust structural optimization", *Engineering Computations*, Vol. 32 No 2, pp.258 - 288.
- Nayfeh A.H., Younis M.I., Abdel-Rahman E.M. (2005), "Reduced-Order Models for MEMS Applications", *Nonlinear Dynamics*, Vol. 41, pp. 211-236.
- Newmark N. (1959), "A method of computation for structural dynamics", *Journal of the Engineering Mechanics Division, ASCE*, Vol. 85 No. 7, pp. 67-94.
- Nour O.B., Clough R.W. (1983), "Dynamic analysis of structures using Lanczos coordinates", *UC Berkeley, Center for Pure and Applied Mathematics*.
- Ohayon R., Soize C. (2014), "Clarification about Component Mode Synthesis Methods for Substructures with Physical Flexible Interfaces, Review Paper", *International Journal of Aeronautical and Space Sciences*, Vol. 15 No. 2, pp. 113-122.
- Perdahcioglu D.A., Ellenbroek M.H.M., De Boer A. (2009), "A hybrid design optimization method using enriched Craig-Bampton approach", *International Congress of Sound and Vibration ICSV16*, July 5-9, Krakow, Poland.
- Perkó Z., Gilli L., Lathouwers D., Kloosterman J.L. (2014), "Grid and basis adaptive polynomial chaos techniques for sensitivity and uncertainty analysis", *Journal of Computational Physics*, Vol. 260, pp. 54-84.
- Raisee M., Kumar D., Lacor C. (2013) "Stochastic Model Reduction for Polynomial Chaos Expansion Using Proper Orthogonal Decomposition", *Chaotic Modeling and Simulation (CMSIM)*, Vol. 4, pp. 615-623.
- Rubinstein R.-Y. (1981), "*Simulation and the Monte Carlo methods*", John Wiley & Sons.
- Sarsri D., Azrar L., Jebbouri A., El Hami A. (2011), "Component mode synthesis and polynomial chaos expansions for stochastic frequency functions of large linear FE models", *Computers & Structures*, Vol. 89, pp. 346-356.
- Schobi R., Sudret B., Wiart J. (2015), "Polynomial-Chaos-Based Kriging", *International Journal of Uncertainty Quantification*, Vol. 5 No. 2, pp. 171-193.
- Sinou J.-J., Didier J., Faverjon B. (2015), "Stochastic nonlinear response of a flexible rotor with local nonlinearities", *International Journal of Non Linear Mechanics*, Vol. 74, pp. 92-99.
- Smallwood D.O. (1994) "Characterization and simulation of transient vibrations using band limited moments", *Shock and Vibration*, Vol. 1 No 6, pp. 507-527.
- Soize C. (2010), "Some aspects of probabilistic modeling, identification and propagation of uncertainties in computational mechanics", *European Journal of Computational Mechanics*, Vol. 19, Giens 2010, pp. 25-40.
- Soize C., Ghanem R. (2004), "Physical systems with random uncertainties: Chaos representations with arbitrary probability measure", *SIAM Journal on Scientific Computing*, Vol. 26 No. 2, pp. 395-410.
- Sudret B. (2007), "Uncertainty propagation and sensitivity analysis in mechanical models: Contribution to structural reliability and stochastic spectral methods", Habilitation thesis: University of BLAISE PASCAL-Clermont II, France.
- Sudret B. (2008), "Global sensitivity analysis using polynomial chaos expansions", *Reliability Engineering & System Safety*, Vol. 93, pp. 964-979.

- Sudret B., Mai C.V. (2015) "Computing derivative based global sensitivity measures using Polynomial chaos expansions", *Reliability Engineering and System Safety*, Vol. 134, pp. 241-250.
- Wan X., Karniadakis G.E. (2005), "An adaptive multi-element generalized polynomial chaos method for stochastic differential equations", *Journal of Computational Physics*, Vol. 209, pp. 617-642.
- Weickum G., Eldred M.S., Maute K. (2009), "A multi-point reduced-order modeling approach of transient structural dynamics with application to reliability-based design optimization", *Structural and Multidisciplinary Optimization*, Vol. 38 No. 6, pp. 599-611.
- Wenneker F., Tiso P. (2014), "A substructuring method for geometrically nonlinear structures", *Dynamics of Coupled Structures*, Vol. 1, pp. 157-165.
- Wiener N. (1938), "The Homogeneous Chaos", *American Journal of Mathematics*, Vol. 60 No. 4, pp. 897-93.
- Xiu D., Karniadakis G.E. (2002), "The Wiener-Askey polynomial chaos for stochastic differential equations", *SIAM Journal on Scientific Computing*, Vol. 24 No. 2, pp. 619-644.
- Yao W., Liou M.-S. (2012), "Reduced-order modeling for flutter/LCO using recurrent artificial neural network", *In 12<sup>th</sup> AIAA Aviation Technology, Integration, and Operations (ATIO) Conference and 14<sup>th</sup> AIAA/ISSM.*

### Biographies:

**Khaoula Chikhaoui** graduated in 2013 with a master diploma from the National High School of Engineers of Tunis (ENSIT). Currently, she is a Ph.D. student under joint supervision between the University of Franche-Comté and the University of Tunis. Her Ph.D. thesis mainly focuses on robust design of periodic structures with functional nonlinearities. Her current research interests include Robust Design, Uncertainty Propagation, Model Reduction and Nonlinear Dynamics.

**Noureddine Bouhaddi** graduated in 1986 with an engineering diploma of Ecole Nationale Supérieure de Mécanique et des Microtechniques (ENSM). After completing his Ph.D in 1992, he became an associate professor at the University of Franche-Comté. Since September 2000, he is a Full Professor at the University of Franche-Comté where he was director of the department of applied mechanics during four years and responsible of a master of engineering since 2004. His area of expertise and current research interests include Models Reduction, Robust Design, Structural Dynamics, Multi-objective Optimization and Vibration Energy Harvesting..

**Najib Kacem** graduated in 2006 with an Arts et Métiers ParisTech (ENSAM) engineering diploma. He joined the French Alternative Energies and Atomic Energy Commission (CEA) in Grenoble to prepare for a Ph.D that he completed in 2010. He subsequently undertook a post-doctoral research position at the University of Geneva (Switzerland). Since September 2011, he is Associate Professor at the University of Franche-Comté. His area of expertise and current research interests include MEMS/NEMS, Nonlinear Dynamics, Energy Harvesting, and Smart Systems.

**Mohamed Guedri** graduated in 2006 with a Ph.D from the university of Tunis. Since 2012, he is Associate Professor at National High School of Engineers of Tunis (ENSIT). His area of expertise and current research interests include Model Reduction, Robust Design and reliability.

**Mohamed Soula** graduated in 1996 with a Ph.D from the Paris-CNAM. Currently, he is an associate professor at University of Tunis. His area of expertise and current research interests include Structural Dynamics, Physics and Materials Science.

## LISTE OF FIGURES

**Fig. 1.** 2D frame structure

**Fig. 2.** MAC matrix comparing the deterministic modes and the mean of the stochastic modes

**Fig. 3.** Mean of the stochastic displacements computed with the full model (LHS-REF) compared to the deterministic model at the observation dofs: (a)  $P_{O1}$  and (b)  $P_{O2}$

**Fig. 4.** Mean of the stochastic displacements computed using the EB (LHS-EB), the standard truncated modal basis (LHS-MB) and the full model (LHS-REF) at the observation dofs: (a)  $P_{O1}$  and (b)  $P_{O2}$

**Fig. 5.** Mean of the stochastic phase diagrams computed using the EB (LHS-EB), the standard truncated modal basis (LHS-MB) and the full model (LHS-REF) at the observation dofs: (a)  $P_{O1}$  and (b)  $P_{O2}$

**Fig. 6.** Mean of the stochastic displacements, at the observation dofs: (a)  $P_{O1}$  and (b)  $P_{O2}$ , computed using the LHS method (LHS-REF) and the gPCE method, of orders 2 (gPC-2-REF) and 6 (gPC-6-REF), on the full model

**Fig. 7.** Mean of the stochastic phase diagrams, at the observation dofs: (a)  $P_{O1}$  and (b)  $P_{O2}$ , computed using the LHS method (LHS-REF) and the gPCE method, of orders 2 (gPC-2-REF) and 6 (gPC-6-REF), on the full model

**Fig. 8.** Mean of the stochastic displacements, at the observation dofs: (a)  $P_{O1}$  and (b)  $P_{O2}$ , computed on the full model using LHS method (LHS-REF) and the sixth order gPCE method on the full (gPC-REF) and the reduced (gPC-EB) models

**Fig. 9.** Mean of the stochastic phase diagrams, at the observation dofs: (a)  $P_{O1}$  and (b)  $P_{O2}$ , computed on the full model using LHS method (LHS-REF) and the sixth order gPCE method on the full (gPC-REF) and the reduced (gPC-EB) models

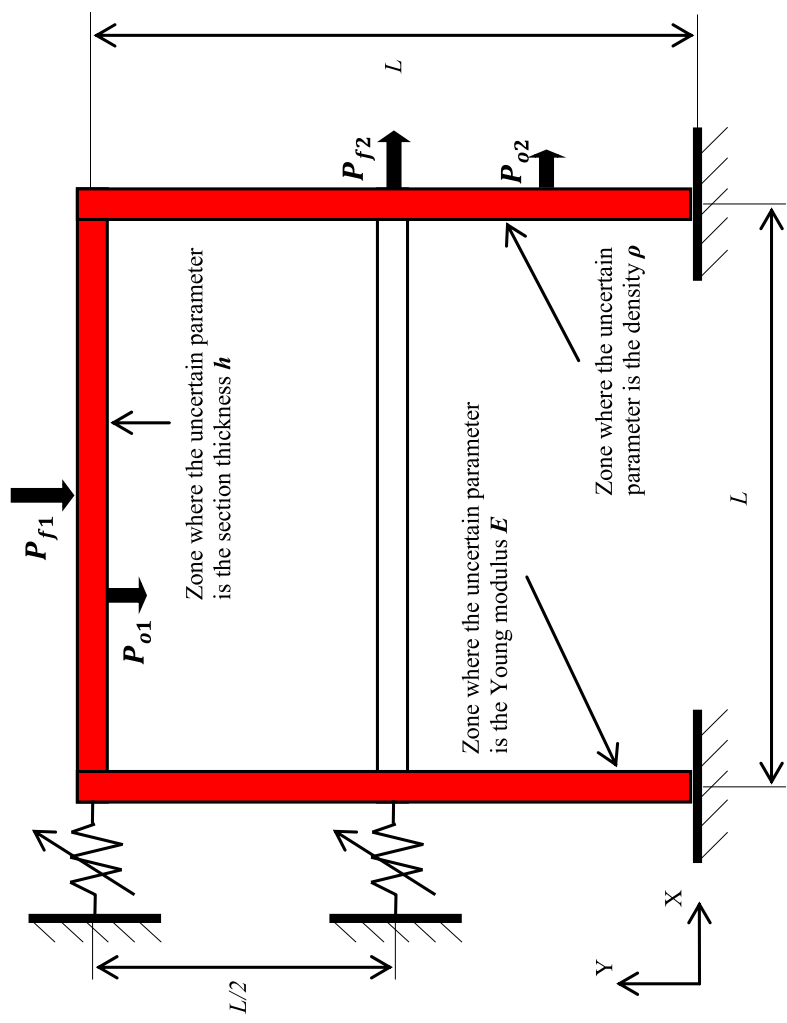
**Fig. 10.** Coupled micro-beams structure

**Fig. 11.** MAC matrix comparing deterministic normal modes and the means of the stochastic modes

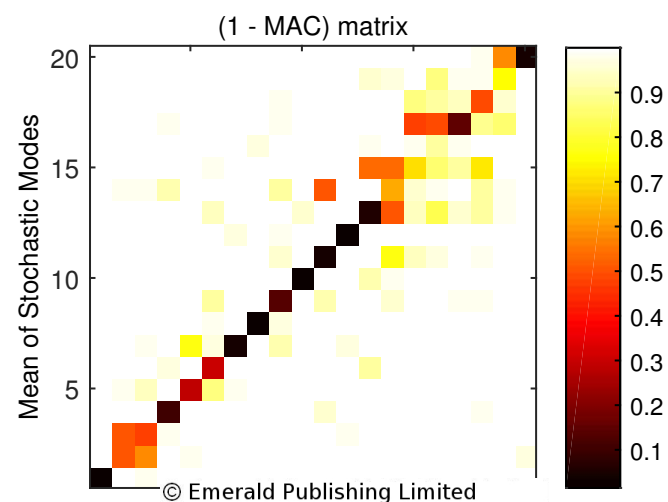
**Fig. 12.** Mean of the stochastic velocities and phase diagrams, at the observation dofs: (a)  $PO_1$  and (b)  $PO_2$ , computed using the LHS method on the full (LHS-REF) and the reduced (LHS-ECBT) models

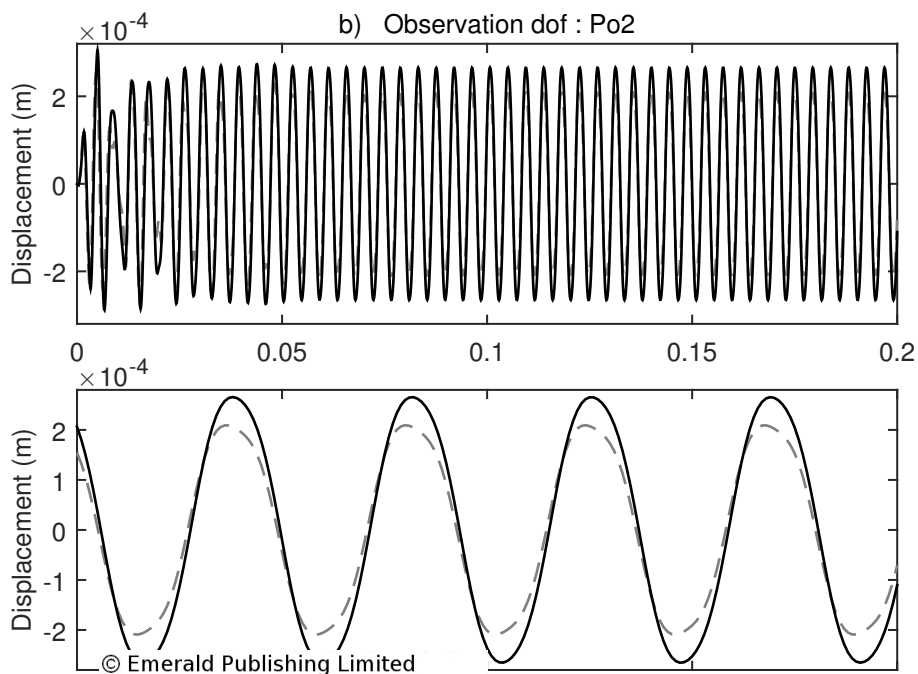
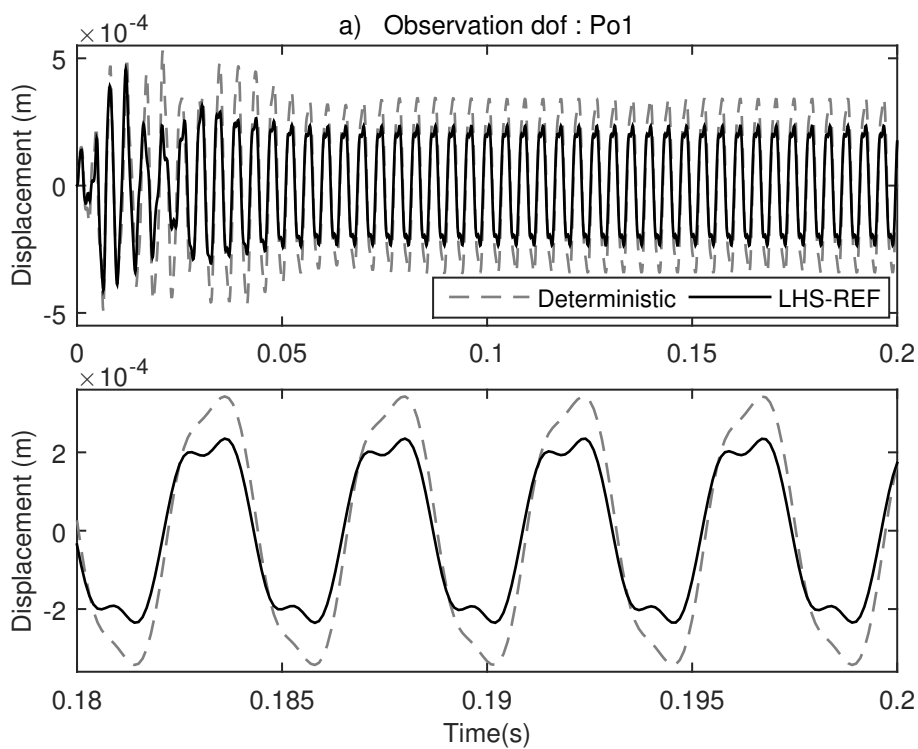
**Fig. 13.** Mean of the stochastic velocities and phase diagrams, at the observation dofs: (a)  $PO_1$  and (b)  $PO_2$ , computed using the gPC method on the full (gPC-REF) and the reduced (gPC-ECBT) models and using the LHS method on the full model

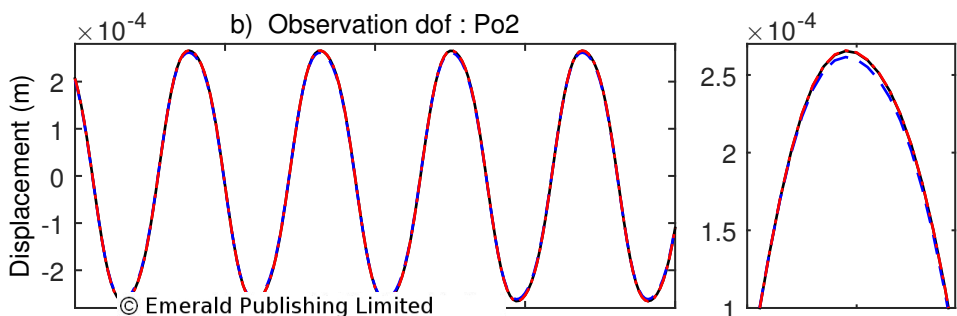
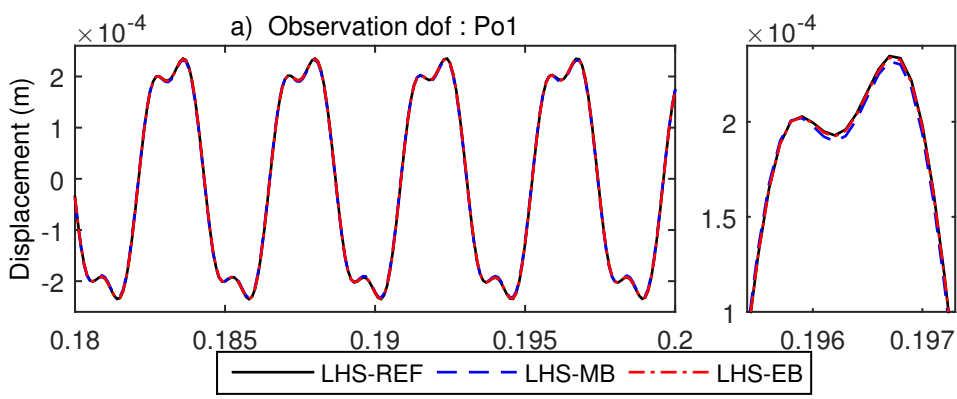
**Fig. 14.** Summary scheme of proposed metamodels

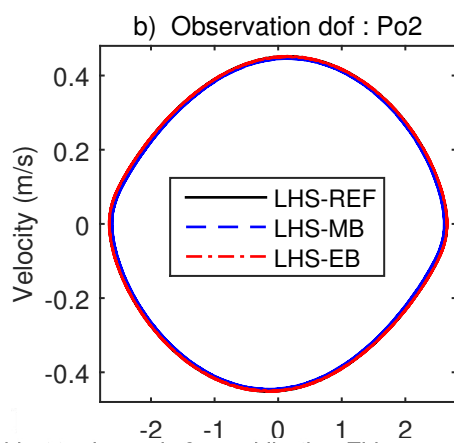
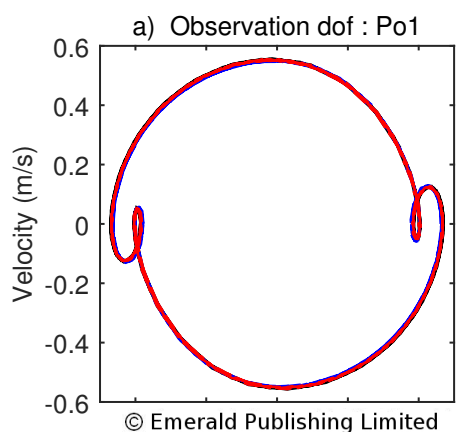


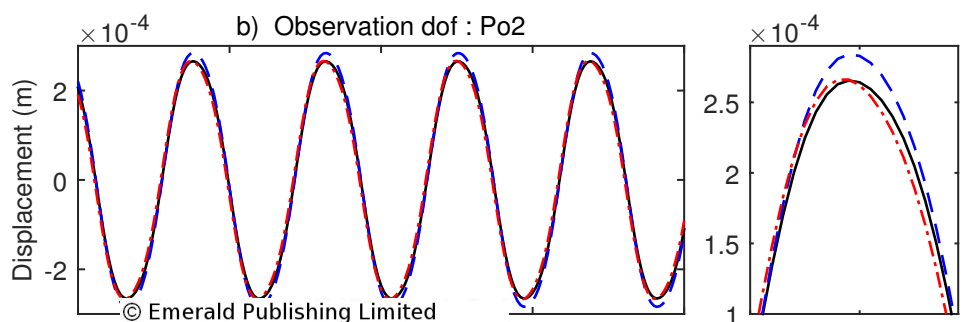
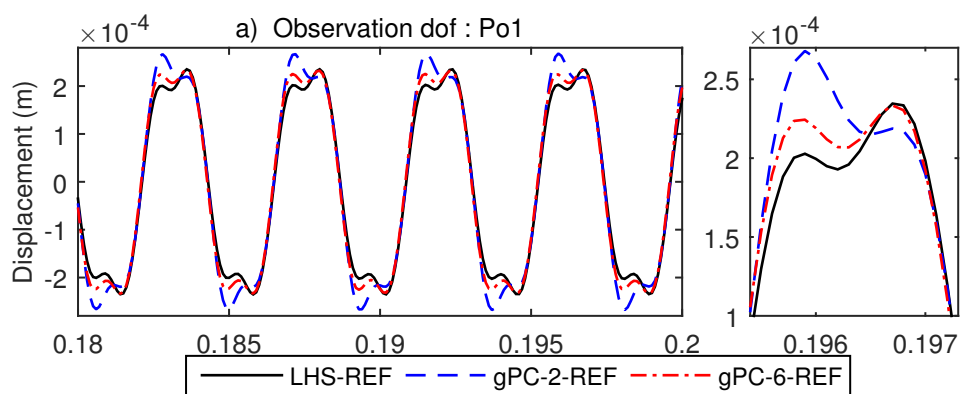


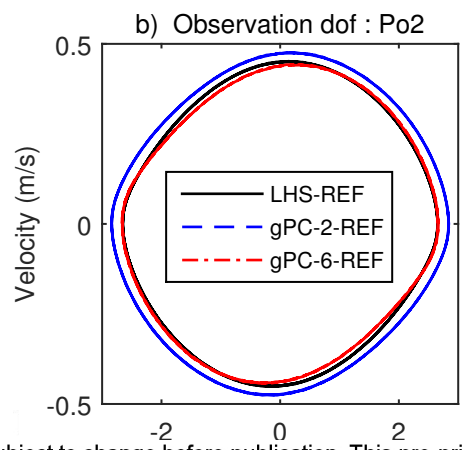
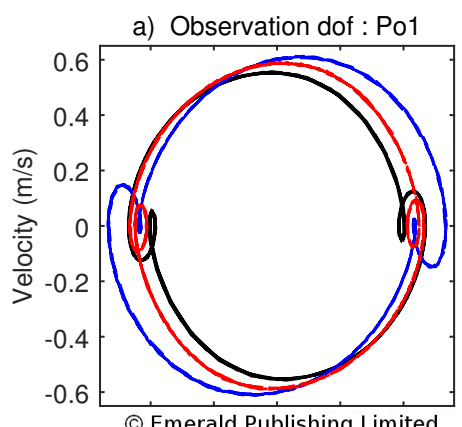


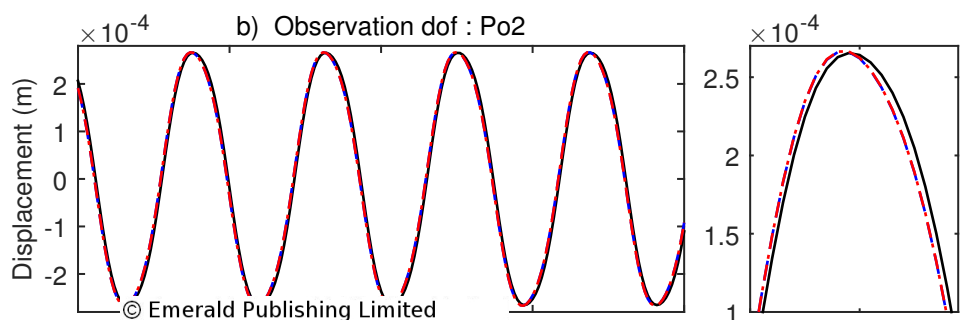
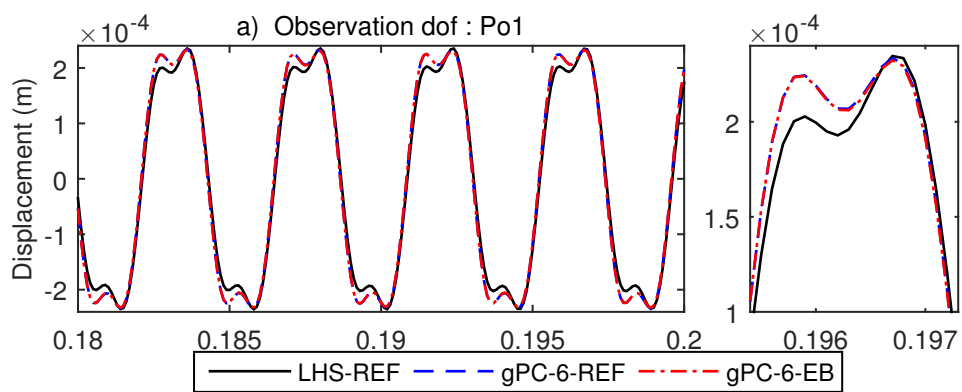


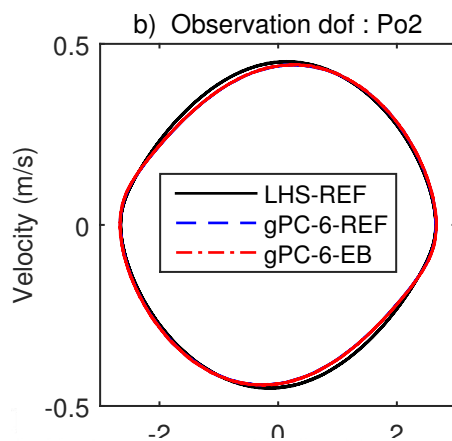
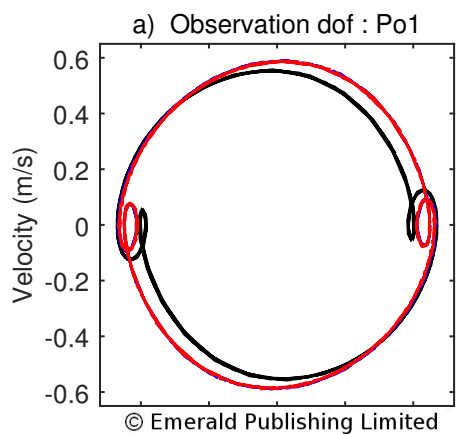




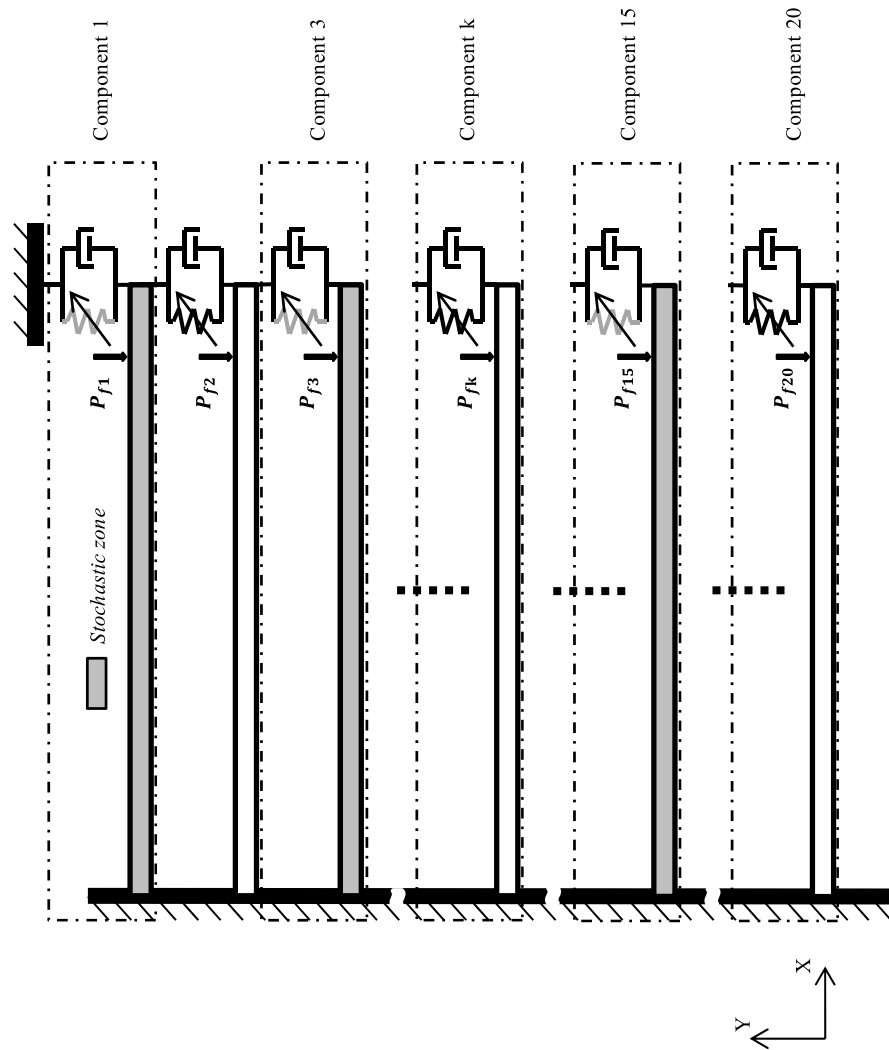


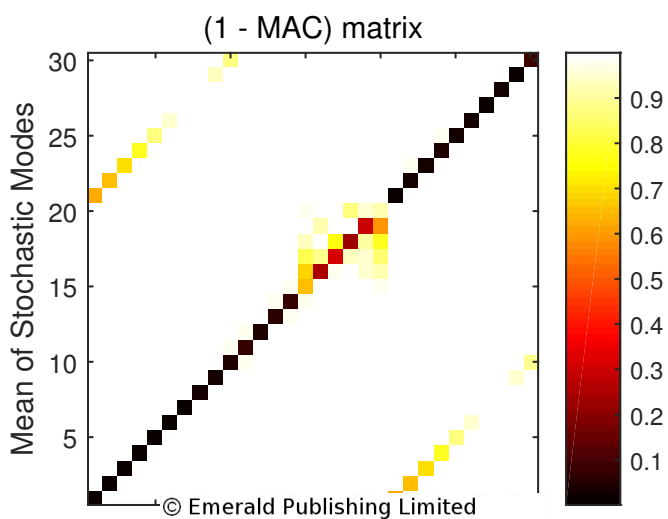




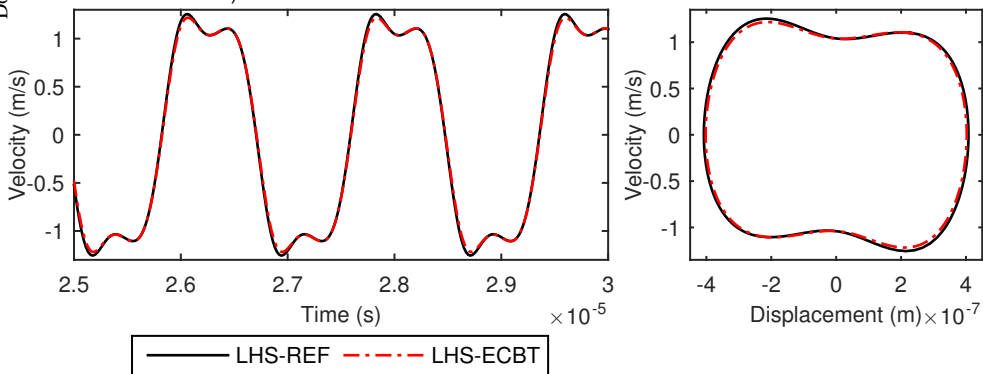




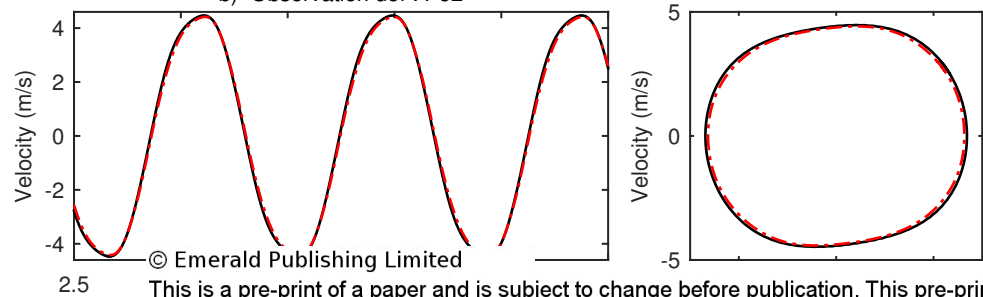




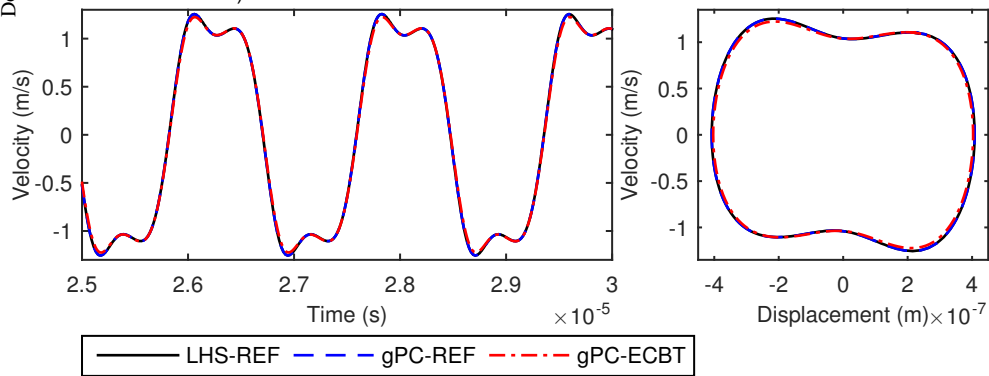
a) Observation dof : Po1



b) Observation dof : Po2



a) Observation dof : Po1



b) Observation dof : Po2

